NASA Technical Paper 1123

Gaussian Step-Pressure Loading of Rigid Viscoplastic Plates

Robert J. Hayduk and Barbara J. Durling

MARCH 1978

NASA

NASA Technical Paper 1123

Gaussian Step-Pressure Loading of Rigid Viscoplastic Plates

Robert J. Hayduk and Barbara J. Durling
Langley Research Center
Hampton, Virginia

National Aeronautics
and Space Administration

**Scientific and Technical
Information Office**

1978

SUMMARY

The response of a thin, rigid viscoplastic plate subjected to a spatially axisymmetric Gaussian step-pressure impulse loading was studied analytically. A Gaussian pressure distribution in excess of the collapse load is applied to the plate, is held constant for a length of time, and then is suddenly removed. The plate deforms with monotonically increasing deflections until the dynamic energy is completely dissipated in plastic work. The simply supported plate of uniform thickness obeys the von Mises yield criterion and a generalized constitutive equation for rigid viscoplastic materials. For the small deflection bending response of the plate, the governing system of equations is essentially nonlinear. Transverse shear stress is neglected in the yield condition and rotary inertia in the equations of dynamic equilibrium. A proportional loading technique, known to give excellent approximations of the exact solution for the uniform load case, was used to linearize the problem and obtain the analytical solutions in the form of eigenvalue expansions. The linearized governing equation required the knowledge of the collapse load of the corresponding static problem.

The effects of load concentration, an order of magnitude change in the viscosity of the plate material, and load duration were examined while holding the total impulse constant. In general, as the load became more concentrated, both the peak central velocity and the time for plate motion to cease increased. For the less viscous plate, these increases of velocity and time were more pronounced. The final plate profile became more conical as the load concentration increased but did not approach the purely conical shape predicted for the ideal point impulse by the rigid perfectly plastic analysis with the Tresca yield criteria. Profiles of the less viscous plate were influenced more by the load concentration. The shorter the time of load application, the greater the initial kinetic energy, the plate response, and the final deformation.

INTRODUCTION

There have been a number of plastic circular plate analyses (refs. 1, 2, and 3) which permit a time variation of the load; however, there have been few papers which consider a radial variation other than linear (refs. 3 and 4). Florence's solutions (ref. 5) for uniform pressure acting over a central region permit one to vary a single parameter to obtain all intermediate states between the point load and uniform distribution. The only other general spatial distribution of load which has received significant analytical attention is the Gaussian distribution. By varying a single parameter, this general distribution can span the extremes from the point load to the uniformly distributed load. This versatility was recognized by Sneddon (ref. 6) who approximated the dynamic loading of a projectile on a thin, infinite elastic plate by a Gaussian distribution of pressure. Madden (ref. 7), in his study of shielding of space vehicle structures against meteoroid penetration, related the meteoroid-shield debris loading

of the main vehicle wall to a Gaussian initial velocity distribution. The first study of this loading on a plastic plate was made by Thomson (ref. 8). He obtained the solution for a rigid, perfectly plastic plate obeying the Tresca yield condition subjected to an ideal impulse of Gaussian distribution. The corresponding solution for the rigid viscoplastic plate obeying the von Mises yield condition is presented in reference 9. Weidman (ref. 2), in considering the response of simply supported circular plastic plates to distributed time-varying loadings, presented an example of a radial Gaussian distribution of pressure with an exponential decay. The plate material in reference 2 was also rigid, perfectly plastic obeying the Tresca yield condition. An approximate solution for a uniformly distributed load acting over a circular region of radius a, assuming a Gaussian distribution of velocity at all time, was obtained by Lepik (ref. 10).

The present paper presents the analytical results for the small deflection bending response of a simply supported circular plate of rigid viscoplastic material. The plate is subjected to a spatially axisymmetric Gaussian distribution of pressure having a rectangular pulse in time. (The corresponding solution for a Gaussian ideal impulse loading is presented in ref. 9.) The effects of load concentration, of an order of magnitude change in the viscosity of the plate material, and of load duration are examined while holding the total impulse constant. Approximate expressions are developed for the time at which plate motion ceases, for the final shape of the plate, and for the final central displacement.

Part of the information presented in this report was included in a thesis entitled "Gaussian Impulsive Loading of Rigid Viscoplastic Plates" submitted by Robert J. Hayduk in partial fulfillment of the requirements for the Degree of Doctor of Philosophy in Engineering Mechanics, Virginia Polytechnic Institute and State University, Blacksburg, Virginia, August 1972.

SYMBOLS

A_n series coefficients, equation (A6)

C_1, C_2 constants defined by equations (A5)

F nondimensional load amplitude, $\frac{\sqrt{3}p_o R^2}{4M_o}$

f yield function

h plate half-thickness

$J_p(x), I_p(x)$ Bessel function of first kind of real and imaginary arguments, respectively

J_2' second invariant of deviatoric stress tensor

$\dot{K}_r, \dot{K}_\phi$ radial and circumferential curvature rates

k	yield stress in simple shear
M_o	yield moment of plate, $\sigma_o h^2$
M_r, M_ϕ	radial and circumferential bending-moment resultants
$\bar{M}_r, \bar{M}_\phi$	radial and circumferential bending-moment resultants at initial yield
m	nondimensional radial bending-moment resultant, M_r/M_o
n	nondimensional circumferential bending-moment resultant, M_ϕ/M_o
$\frac{P'}{\pi M_o}$	total nondimensional load-carrying capacity, $\frac{p_o' R^2}{M_o}\left(\frac{1 - e^{-\beta}}{\beta}\right)$
p_o	pressure amplitude at plate center
$\bar{p}_o$	nondimensional pressure amplitude at plate center, $p_o R^2/M_o$
Q	shear stress resultant
q	nondimensional shear stress resultant, RQ/M_o
R	plate radius
r	radial coordinate
S_{ij}	deviator stress tensor
$\bar{S}_{ij}$	deviator stress tensor at initial yield
t	time
t_f	time for motion to cease
$U(\rho)$	steady component of velocity
$u(\rho,t)$	dynamic component of velocity
v	nondimensional plate velocity, $\frac{\mu R^2}{\alpha M_o}\frac{\partial w}{\partial t}$
w	transverse deflection of plate
z	transverse coordinate
α	plate geometry and material constant, $\frac{\sqrt{3}\mu R^4 \gamma}{2hM_o}$, sec
β	nondimensional Gaussian shape parameter
γ	material constant, $\gamma^o/2k$

γ^o	material constant
$\dot{\epsilon}_{ij}$	strain rate tensor
λ_n	eigenvalues determined from equation (A7)
μ	mass density per unit area of plate
ρ	nondimensional radial coordinate, r/R
σ_{ij}	stress tensor
σ_o	yield stress in simple tension
τ	load duration, sec
$\Phi(f)$	function defined by equations (3)
ϕ	circumferential coordinate
$\phi(\lambda_n,\beta)$	function defined by equation (A13)
$\psi(\lambda_n,\rho,\beta)$	function defined by equation (A12)
∇^2,∇^4	harmonic and biharmonic operators in cylindrical coordinates

LINEARIZATION OF THE GENERALIZED CONSTITUTIVE EQUATIONS FOR RIGID VISCOPLASTIC MATERIALS

A generalized constitutive equation for rigid viscoplastic materials is presented in this section. Material elasticity is neglected in order to simplify the analysis as is frequently done in theoretical investigations of dynamic plastic response of structures. Such an assumption is generally believed to be valid when the dynamic energy is considerably larger than the maximum energy which could be absorbed in a wholly elastic manner and the duration of loading is short compared with the fundamental period of vibration.

Perzyna (ref. 11) developed a constitutive equation for rate-sensitive plastic materials by generalizing the constitutive relationships used by previous researchers (Hohenemser and Prager in ref. 12; and Prager in ref. 13). The generalized constitutive equation proposed by Perzyna is

$$\dot{\epsilon}_{ij} = \gamma^o \Phi(f) \frac{\partial f}{\partial \sigma_{ij}} \tag{1}$$

where $\dot{\epsilon}_{ij}$ is the strain rate tensor and

$$f = \frac{J_2'^{1/2}}{k} - 1 \tag{2}$$

The second invariant of the deviatoric stress tensor is

$$J_2' = \frac{1}{2} S_{ij}S_{ij}$$

where

$$S_{ij} = \sigma_{ij} - \frac{1}{3} \delta_{ij}\sigma_{kk}$$

The function in the generalized constitutive equation (eq. (1)) is defined as

$$\left.\begin{aligned} \Phi(f) &= 0 \qquad (f \leq 0) \\ \Phi(f) &\neq 0 \qquad (f > 0) \end{aligned}\right\} \tag{3}$$

Also, k is the yield stress in simple shear and γ^o denotes a physical constant of the material.

Perzyna (ref. 14) has shown that the generalized constitutive equation for viscoplastic materials reduces to the constitutive equations of an incompressible, perfectly plastic material first considered by von Mises and to the flow law of perfect plasticity theory. As in the theory of perfectly plastic solids, convexity of the subsequent dynamic loading surfaces and orthogonality of the inelastic strain-rate vector to the yield surface follow from Drucker's postulates defining a stable inelastic material with inclusion of time-dependent terms (ref. 11).

A method of linearizing boundary-value problems in the theory of viscoplastic solids is described by Wiezbicki in reference 15. In this method, as shown graphically in figure 1, the concept of proportional loading is used to relate the state of stress S_{ij} in the subsequent stress state to the state of stress $\bar{S}_{ij}$ on the initial yield surface $f = 0$. For proportional loading the direction cosine tensor of the state of stress in deviatoric space is independent of time. The proportional loading that satisfies equation (2) is given by

$$S_{ij} = \frac{J_2'^{1/2}}{k} \bar{S}_{ij} \tag{4}$$

This equation is a reasonable approximation for axisymmetrically loaded, simply supported circular plates because the plate center and boundary are automatically proportionally loaded; that is, the bending moments must always be equal at the plate center and the radial bending moment must always be zero at the plate boundary.

When equation (4) is utilized, the generalized constitutive equation (eq. (1)) becomes

$$\dot{\epsilon}_{ij} = \frac{\gamma}{k} \Phi(f) \bar{S}_{ij} \tag{5}$$

where the viscosity constant γ equals $\gamma^o/2k$ and $f = \frac{S_{ij}}{\bar{S}_{ij}} - 1$. The ratio $S_{ij}/\bar{S}_{ij}$ may be expressed in terms of any one of the deviatoric stress components. The simplified constitutive equation (eq. (5)) still is nonlinear in stresses. However, for this analysis, the linear form

$$\Phi(f) = f \tag{6}$$

is chosen to produce full linearization of the constitutive equation (eq. (5)) as follows:

$$\dot{\epsilon}_{ij} = \frac{\gamma}{k}(S_{ij} - \bar{S}_{ij}) \tag{7}$$

It should be noted that equation (7) is really a flow relation for a given structure rather than a constitutive equation describing a given material (ref. 16).

For the problem of a uniformly loaded, simply supported circular plate with $\Phi(f) = f$, Wierzbicki (ref. 15) has shown that the approximate solution, obtained with the proportional loading hypothesis, agrees very well with a numerical finite-difference solution without the proportional loading approximation. The solution of the linearized problem also agrees well with experimental data on impulsively loaded plates obtained by Florence (ref. 17).

GOVERNING EQUATIONS AND BOUNDARY AND INITIAL CONDITIONS

A Gaussian transverse load, described by

$$p(r) = p_o e^{-\beta r^2/R^2} \tag{8}$$

is suddenly applied to the entire surface of a rigid viscoplastic plate of radius R and thickness $2h$, where β is a nondimensional load shape parameter. The boundary of the plate at $r = R$ is simply supported. After being applied steadily during the time interval $0 \leq t \leq \tau$, the load is suddenly removed. The geometry of the plate and loading are shown in figure 2. For $\beta = 0$, equation (8) describes a uniform load; as β approaches ∞ and p_o approaches ∞, equation (8) describes a point load at the plate center.

In the derivation that follows, the equations apply to the loading phase $0 \leq t \leq \tau$. To obtain the equations for the postload phase $t > \tau$, the applied load terms must be omitted. The internal forces and moments acting on a typical plate element are shown in figure 3. If rotary inertia is neglected but transverse inertia is taken into account, the equations of motion are

$$\left.\begin{aligned} \frac{\partial}{\partial r}(rQ) + rp_o e^{-\beta r^2/R^2} &= \mu r \frac{\partial^2 w}{\partial t^2} \\ \frac{\partial}{\partial r}(rM_r) - M_\phi &= rQ \end{aligned}\right\} \tag{9}$$

With the usual assumptions of small deflection plate theory - that is, plane sections remain plane, strains vary linearly through the thickness, and strains are linearly related to the curvature - the curvature-rate—moment relations, derived from the linearized constitutive equation (eq. (7)), are

$$\left.\begin{aligned} \dot{K}_r &= \frac{\sqrt{3}\gamma}{2hM_o}\left[(2M_r - M_\phi) - (2\bar{M}_r - \bar{M}_\phi)\right] \\ \dot{K}_\phi &= \frac{\sqrt{3}\gamma}{2hM_o}\left[(2M_\phi - M_r) - (2\bar{M}_\phi - \bar{M}_r)\right] \end{aligned}\right\} \tag{10}$$

The moments $\bar{M}_r$ and $\bar{M}_\phi$ satisfy, for any value of r, the equation of the initial yield surface,

$$\bar{M}_r^2 - \bar{M}_r\bar{M}_\phi + \bar{M}_\phi^2 = M_o^2 \tag{11}$$

where $M_o = \sigma_o h^2$ is the yield moment of the plate material and $\sigma_o = \sqrt{3}k$ is the yield stress in simple tension.

For small deflections of the plate, the curvature rates $\dot{K}_r$ and $\dot{K}_\phi$ are related to the deflection rate $\dot{w}$ by

$$\left.\begin{aligned} \dot{K}_r &= -\frac{\partial^2\dot{w}}{\partial r^2} \\ \dot{K}_\phi &= -\frac{1}{r}\frac{\partial\dot{w}}{\partial r} \end{aligned}\right\} \tag{12}$$

Equations (9), (10), and (12) form a linear parabolic system of partial differential equations with six unknown functions - M_r, M_ϕ, Q, $\dot{w}$, $\dot{K}_r$, and $\dot{K}_\phi$ - plus the unknown static moment distributions $\bar{M}_r$ and $\bar{M}_\phi$.

By eliminating all unknowns except $\dot{w}$, the system of governing equations can be reduced to the single, fourth-order equation:

$$\frac{4M_o h}{3\sqrt{3}\gamma}\nabla^4\dot{w} - p_o e^{-\beta r^2/R^2} + \mu\frac{\partial\dot{w}}{\partial t} = \frac{1}{r}\frac{\partial}{\partial r}\left[\frac{\partial}{\partial r}(r\bar{M}_r) - \bar{M}_\phi\right] \tag{13}$$

where

$$\nabla^4 = \left[\frac{\partial^2}{\partial r^2} + \frac{1}{r}\frac{\partial}{\partial r}\right]\left[\frac{\partial^2}{\partial r^2} + \frac{1}{r}\frac{\partial}{\partial r}\right]$$

The right-hand side of equation (13) represents the internal force distribution in the plate at the initiation of collapse for the static case.

Let p_o' denote the amplitude of the static load-carrying capacity of the plate, then the right-hand side of equation (13) can be replaced by $-p_o' e^{-\beta r^2/R^2}$ and the governing equation becomes

$$\frac{4M_o h}{3\sqrt{3}\gamma}\nabla^4\dot{w} + \mu\frac{\partial\dot{w}}{\partial t} = (p_o - p_o')e^{-\beta r^2/R^2} \tag{14}$$

This method of solution, proposed by Wierzbicki (ref. 15), has the important property of replacing the unknown static moment distributions $\bar{M}_r$ and $\bar{M}_\phi$, whose explicit formulas are not known for the von Mises yield condition, by the load distribution at initiation of static collapse, that is, $p_o'e^{-\beta r^2/R^2}$. Thus, the need for explicit formulas has been reduced to finding the value of a constant p_o' corresponding to a particular value of the shape parameter β. The determination of the load-carrying capacity of a circular plate under a Gaussian distribution of pressure is presented in reference 18. For completeness the variation of p_o' and total nondimensional load-carrying capacity,

$$\frac{P'}{\pi M_o} = \frac{p_o' R^2}{M_o}\left(\frac{1 - e^{-\beta}}{\beta}\right)$$

obtained by integrating the pressure distribution over the plate, are shown as functions of β in figure 4.

Define the nondimensional quantities as

$$\left.\begin{aligned} m &= \frac{M_r}{M_o} \qquad n = \frac{M_\phi}{M_o} \qquad q = \frac{RQ}{M_o} \qquad \rho = \frac{r}{R} \\ v &= \frac{\mu R^2}{\alpha M_o}\frac{\partial w}{\partial t} \qquad F = \frac{\sqrt{3}p_o R^2}{4M_o} \qquad F' = \frac{\sqrt{3}p_o' R^2}{4M_o} \end{aligned}\right\} \tag{15}$$

and let $\nabla^2 = \frac{\partial^2}{\partial\rho^2} + \frac{1}{\rho}\frac{\partial}{\partial\rho}$; then the final form of the governing equation (eq. (14)) is

$$\nabla^4 v + \frac{3}{2}\alpha\frac{\partial v}{\partial t} = 2\sqrt{3}(F - F')e^{-\beta\rho^2} \tag{16}$$

where

$$\alpha = \frac{\sqrt{3}\gamma\mu R^4}{2hM_o}$$

The boundary conditions of the simply supported plate are

$$\left.\begin{aligned} m = n \quad \text{and} \quad q = 0 \qquad (\rho = 0) \\ v = m = 0 \qquad (\rho = 1) \end{aligned}\right\} \tag{17}$$

By using equations (10), (12), and (9), equations (17), in terms of rate of deflection, become

$$\lim_{\rho\to 0}\left(\frac{\partial^2 v}{\partial\rho^2} - \frac{1}{\rho}\frac{\partial v}{\partial\rho}\right) = 0 \tag{18a}$$

$$\lim_{\rho \to 0}\left(\frac{\partial^3 v}{\partial \rho^3} + \frac{1}{\rho}\frac{\partial^2 v}{\partial \rho^2} - \frac{1}{\rho^2}\frac{\partial v}{\partial \rho}\right) = 0 \tag{18b}$$

$$2\frac{\partial^2 v}{\partial \rho^2} + \frac{1}{\rho}\frac{\partial v}{\partial \rho}\bigg|_{\rho=1} = 0 \tag{18c}$$

$$v(1,t) = 0 \tag{18d}$$

For the Gaussian step-pressure loading, the plate is initially flat and at rest; that is,

$$w(\rho,0) = 0 \qquad v(\rho,0) = 0 \tag{19}$$

RESULTS AND DISCUSSION

The solution to the governing equation (eq. (16)) with associated boundary and initial conditions (eqs. (18) and (19)) is presented in the appendix. Effects of load distribution and plate viscosity on plate response are examined while holding the load duration τ and the total impulse $I_T = \pi R^2 \tau p_o \beta^{-1}(1 - e^{-\beta})$ constant. The constants used in the graphical presentations were chosen to be consistent with results of reference 15; that is, $\tau = 0.1$ msec and $(\bar{p}_o)_{\beta=0} = \dfrac{(\bar{p}_o)_{\beta=0} R^2}{M_o} = 10$. Values of α of 1×10^{-3} and 1×10^{-2} sec are used to show effects of plate material viscosity. Effects of load distribution are given by the parameter β. The required variation of $\bar{p}_o$ with β in order to maintain constant total impulse is given by the parameter

$$F = \frac{\sqrt{3}}{4}(\bar{p}_o)_{\beta=0}\frac{\beta}{1 - e^{-\beta}} \tag{20}$$

The values of F determined from equation (20) and used in the computations are

β	F
0	4.33013
10^{-3}	4.33229
1	6.85016
10	43.3032
100	433.013
10 000	43 301.3

The load becomes more concentrated at the center of the plate as β is increased and the amplitude increases almost linearly as β becomes large. The graphical results were obtained by programing the modal solution as given in the appendix (eqs. (A14), (A15), (A17), and (A18)).

In figure 5, the time histories of the plate central velocity for β ranging from 10^{-3} to 10 000 are shown collectively for the two values of the parameter α. The effect of varying the shape of the load from a uniform one to essentially a point load is seen immediately. The peak velocity, which occurs at the instant of load removal, is increased tremendously - a factor of approximately 6 for $\alpha = 1 \times 10^{-3}$ sec and 10 for $\alpha = 1 \times 10^{-2}$ sec. The time for the central velocity to become zero also increased with β, this effect being more pronounced for $\alpha = 1 \times 10^{-2}$ sec.

The results of figure 5 indicate smaller values of nondimensional velocity for $\alpha = 1 \times 10^{-2}$ sec. However, the nondimensional velocity $v(0,t)$ plotted is the actual velocity $\partial w/\partial t$ divided by the constant $\alpha M_o/\mu R^2$. Thus, although the nondimensional value of velocity decreases with an increase in α, the actual velocity increases. For example, for $\beta = 10\ 000$ and $t = \tau$, the curves of figures 5(a) and 5(b) show that

$$\frac{\left[v(0,\tau)\right]_{\alpha=1\times10^{-2}}}{\left[v(0,\tau)\right]_{\alpha=1\times10^{-3}}} \approx 0.291$$

which corresponds to

$$\frac{\left[\frac{\partial w}{\partial t}(0,\tau)\right]_{\alpha=1\times10^{-2}}}{\left[\frac{\partial w}{\partial t}(0,\tau)\right]_{\alpha=1\times10^{-3}}} \approx 2.91$$

Thus, the less viscous plate (the one with the higher value of α and, consequently, the higher value of γ) attains higher velocities, has larger displacements, and acquires more energy from the applied load which requires longer times to dissipate than the more viscous plate.

The profiles of the plate are shown in figure 6 for both values of α and various values of β. As the load becomes more concentrated the profile becomes more conical, as one would expect. Figure 6(b) indicates that the profiles of the less viscous plate are influenced more by the shape parameter β than are those for $\alpha = 1 \times 10^{-3}$ sec.

An approximation of the deflection of the plate is obtained from equation (A18) by retaining only the first term of the series and by using the approximation

$$C_1 + C_2\rho^2 + \frac{1}{2\beta}\, e^{-\beta\rho^2} + \left(\frac{1}{\beta} + \rho^2\right) \sum_{n=1}^{\infty} \frac{(-1)^n(\beta\rho^2)^n}{(2n)n!} \approx -\frac{16\beta}{3}\frac{1}{\lambda_1^5}\,\psi(\lambda_1,\rho,\beta)$$

which is obtained from equation (A14) with $v(\rho,0) = 0$. The result for $\tau < t < t_f$ is

$$\frac{\mu R^2}{\alpha^2 M_o} w(\rho,t) = \frac{\sqrt{3}}{4\beta\alpha}\left[C_1 + C_2\rho^2 + \frac{1}{2\beta}\, e^{-\beta\rho^2} + \left(\frac{1}{\beta} + \rho^2\right) \sum_{n=1}^{\infty} \frac{(-1)^n(\beta\rho^2)^n}{(2n)n!}\right]$$
$$\times \left\{F't - F\tau - \frac{3\alpha}{2\lambda_1^4}\left[(F - F')e^{-(2\lambda_1^4/3\alpha)t}\right.\right.$$
$$\left.\left. - Fe^{-(2\lambda_1^4/3\alpha)(t-\tau)} + F'\right]\right\} \tag{21}$$

An approximate expression for the time for motion to cease can be obtained by setting the derivative of the approximate displacement expression to zero, that is, $\left.\frac{\partial w}{\partial t}\right|_{t_f} = 0$, is

$$t_f = \frac{3\alpha}{2\lambda_1^4} \ln\left[1 + \frac{F}{F'}\left(e^{(2\lambda_1^4/3\alpha)\tau} - 1\right)\right] \tag{22}$$

Equation (22), plotted in figure 7 for $0 \leq \beta \leq 100$ and the two values of α, is an implicit function of β since F and F' vary with β. The effect of β, as shown in figure 7, diminishes after an initial rapid rise of t_f with increasing β. The symbols represent computed times using the complete equation for the velocity (eq. (A17)). Equation (22) is a very good approximation for $\alpha = 1 \times 10^{-3}$ sec; however, except for small values of β, the approximation is poor for $\alpha = 1 \times 10^{-2}$ sec.

The substitution of equation (22) for t_f into equation (21) provides an approximate expression for the final plate displacements

$$\frac{\mu R^2}{\alpha^2 M_o} w(\rho,t_f) = \frac{\sqrt{3}}{4\beta\alpha}\left[C_1 + C_2\rho^2 + \frac{1}{2\beta}\, e^{-\beta\rho^2} + \left(\frac{1}{\beta} + \rho^2\right) \sum_{n=1}^{\infty} \frac{(-1)^n(\beta\rho^2)^n}{(2n)n!}\right]$$
$$\times \left\{F' \frac{3\alpha}{2\lambda_1^4} \ln\left[1 + \frac{F}{F'}\left(e^{(2\lambda_1^4/3\alpha)\tau} - 1\right)\right] - F\tau\right\} \tag{23}$$

and an approximate expression for the final center displacement

$$\frac{\mu R^2}{\alpha^2 M_o} w(0,t_f) = \frac{\sqrt{3}}{4\beta\alpha}\left(C_1 + \frac{1}{2\beta}\right)\left\{F' \frac{3\alpha}{2\lambda_1^4} \ln\left[1 + \frac{F}{F'}\left(e^{(2\lambda_1^4/3\alpha)\tau} - 1\right)\right] - F\tau\right\} \tag{24}$$

Equation (24) is plotted as a function of β for the two values of α in figure 8. The approximations are in excellent agreement with the points computed from the exact equations for both $\alpha = 1 \times 10^{-3}$ sec and 1×10^{-2} sec, although the t_f approximations for the larger value of α were poor for large values of β as shown in figure 7. Again, the nondimensional central displacements are shown smaller for $\alpha = 1 \times 10^{-2}$ sec whereas the actual displacements are larger than for $\alpha = 1 \times 10^{-3}$ sec.

Although not shown, profiles obtained from the approximation (eq. (23)) were compared with profiles obtained from the exact equation (eq. (A18)). For $\alpha = 1 \times 10^{-3}$ sec, the differences between the approximate and exact profiles were negligibly small for the entire range of β considered, 10^{-3} to 10 000. However, for the less viscous plates, $\alpha = 1 \times 10^{-2}$ sec, the differences were not negligible and the approximation (eq. (23)) should therefore be restricted accordingly.

The effect of load duration on the final center displacement is shown in figure 9. Total impulse was held constant as before. For these results the approximate expression (eq. (24)) was used with $\alpha = 1 \times 10^{-3}$ sec and $\beta = 10$. The point $\tau = 0$ represents the ideal impulse and was calculated by using the corresponding approximate center displacement equation of reference 9. As seen in the figure, the center displacement monotonically decreases as the pulse duration lengthens. The maximum center displacement occurs for the ideal impulse. The final center displacement becomes zero at $\tau = 3.32 \times 10^{-4}$ sec, the impulse duration at which the applied load becomes equal to the collapse load of the plate. For impulses beyond that duration, the plate remains rigid.

CONCLUDING REMARKS

A thin, simply supported, rigid, viscoplastic plate subjected to a Gaussian step-pressure impulse loading has been analyzed within the realm of small deflection bending theory. The plate material obeys the von Mises yield criteria and a generalized constitutive equation. These considerations lead, essentially, to nonlinear equations governing the dynamic response of the thin plate. A proportional loading hypothesis, known to give excellent approximations of the exact solution for the uniform load case, was used to linearize the problem and obtain analytical solutions in the form of eigenvalue expansions. The linearized governing equation on the velocity of the plate required the knowledge of the collapse load of the corresponding static problem, that is, the collapse load for the specific load distribution parameter β.

The effects of load concentration, an order of magnitude change in the viscosity of the plate material, and load duration were examined while holding the total impulse constant. In general, as the load became more concentrated, both the peak central velocity and the time for plate motion to cease increased. For the less viscous plate material, these increases of velocity and time for plate motion to cease were more pronounced. The final plate profile became more conical as the load concentration increased but did not approach the purely conical shape predicted by the rigid, perfectly plastic analysis with the Tresca yield condition for an ideal point impulse. As the viscosity of the plate

decreases, the shape parameter has more effect on the final deformed plate profiles.

Approximate expressions were developed for the time at which plate motion ceases, the final shape of the plate, and the final central displacement. Comparisons with the exact series solution indicated that all approximations were excellent for a plate property constant α of 1×10^{-3} sec throughout the range of shape parameter β. For $\alpha = 1 \times 10^{-2}$ sec, the approximation for the final central deflection was good for the entire range of β, but the other approximations were limited in usefulness.

Comparisons between the results of the step-pressure loading and the ideal impulse loading indicate that the viscoplastic plate subjected to a certain total impulse achieves a larger peak velocity and, consequently, kinetic energy if the impulse is delivered instantaneously - that is, as an ideal impulse - rather than over a finite length of time. Consequently, the viscoplastic plate subjected to the ideal impulse requires a longer time after load removal to dissipate its higher energy and experiences larger permanent deflections than the plate subjected to the step-pressure loading of the same total impulse.

Langley Research Center
National Aeronautics and Space Administration
Hampton, VA 23665
February 8, 1978

APPENDIX

SOLUTION OF GOVERNING EQUATION BY EIGENVALUE EXPANSION

The governing equation (eq. (16)) can be solved by means of an eigen expansion method since the right-hand side of the equation is not a function of time. Equation (16) is repeated here for convenience:

$$\nabla^4 v + \frac{3}{2}\alpha\frac{\partial v}{\partial t} = 2\sqrt{3}(F - F')e^{-\beta\rho^2}$$

Substitution of

$$v(\rho,t) = u(\rho,t) + U(\rho) \tag{A1}$$

into equation (16) results in

$$\nabla^4 u(\rho,t) + \frac{3}{2}\alpha\frac{\partial u(\rho,t)}{\partial t} + \nabla^4 U(\rho) = 2\sqrt{3}(F - F')e^{-\beta\rho^2}$$

which separates into

$$\nabla^4 u + \frac{3}{2}\alpha\frac{\partial u}{\partial t} = 0 \tag{A2}$$

and

$$\nabla^4 U = 2\sqrt{3}(F - F')e^{-\beta\rho^2} \tag{A3}$$

Equation (A3) is the same as equation (16) except for the absence of the inertia term. Thus, $U(\rho)$ is an equilibrium solution of equation (16) with the same boundary conditions (eqs. (18)), as follows:

$$U(\rho) = -\frac{\sqrt{3}}{4\beta}(F - F')\left\{C_1 + C_2\rho^2 + \frac{1}{2\beta}e^{-\beta\rho^2} + \left(\frac{1}{\beta} + \rho^2\right)\sum_{m=1}^{\infty}\frac{(-1)^m(\beta\rho^2)^m}{(2m)m!}\right\} \tag{A4}$$

where

$$\left.\begin{aligned} C_1 &= \frac{1}{6\beta} - \frac{7}{6} - \frac{2}{3\beta}e^{-\beta} - \frac{1}{\beta}\sum_{m=1}^{\infty}\frac{(-1)^m\beta^m}{(2m)m!} \\ C_2 &= -\frac{1}{6\beta} + \frac{7}{6} - \frac{1}{6\beta}e^{-\beta} - \sum_{m=1}^{\infty}\frac{(-1)^m\beta^m}{(2m)m!} \end{aligned}\right\} \tag{A5}$$

A general solution due to Wierzbicki (ref. 15) satisfying equation (A2) and all prescribed boundary conditions can be written in the form

APPENDIX

$$u(\rho,t) = \sum_{n=1}^{\infty} A_n\left[I_0(\lambda_n)\ J_0(\lambda_n\rho) - J_0(\lambda_n)\ I_0(\lambda_n\rho)\right]e^{-(2\lambda_n^4/3\alpha)t} \tag{A6}$$

where $J_0(x)$ and $I_0(x)$ denote the Bessel functions of the first kind of real and imaginary arguments. The solution (eq. (A6)) identically satisfies the boundary conditions (eqs. (18a), (18b), and (18d)). The eigenvalues λ_n are roots of the following transcendental equation stemming from the boundary condition (eq. (18c)) of zero bending moment at the plate edge:

$$I_0(\lambda_n)\ J_1(\lambda_n) + I_1(\lambda_n)\ J_0(\lambda_n) - 4\lambda_n\ I_0(\lambda_n)\ J_0(\lambda_n) = 0 \tag{A7}$$

The only remaining unknowns in the solution are the series coefficients A_n. These coefficients are evaluated from the initial condition (eqs. (19)), that is,

$$v(\rho,0) = u(\rho,0) + U(\rho) = 0$$

Thus,

$$u(\rho,0) = -U(\rho) \tag{A8}$$

and substituting equation (A6) for $u(\rho,0)$ gives the following equation:

$$\sum_{n=1}^{\infty} A_n\left[I_0(\lambda_n)\ J_0(\lambda_n\rho) - J_0(\lambda_n)\ I_0(\lambda_n\rho)\right] = -U(\rho) \tag{A9}$$

The coefficients A_n can be determined from equation (A9) by virtue of the orthogonality of the system $\left[I_0(\lambda_n)\ J_0(\lambda_n\rho) - J_0(\lambda_n)\ I_0(\lambda_n\rho)\right]$ on the interval $[0,1]$ where ρ is used as a weighting function. Therefore, coefficients A_n can be determined as

$$A_n = -\frac{\displaystyle\int_0^1 \rho U(\rho)\left[I_0(\lambda_n)\ J_0(\lambda_n\rho) - J_0(\lambda_n)\ I_0(\lambda_n\rho)\right]\,d\rho}{\displaystyle\int_0^1 \rho\left[I_0(\lambda_n)\ J_0(\lambda_n\rho) - J_0(\lambda_n)\ I_0(\lambda_n\rho)\right]^2\,d\rho} \tag{A10}$$

where $U(\rho)$ is defined by equation (A4). The resulting coefficients are

$$A_n\left[I_0(\lambda_n)\ J_0(\lambda_n\rho) - J_0(\lambda_n)\ I_0(\lambda_n\rho)\right] = -\frac{4}{3}(F - F')\frac{1}{\lambda_n^5}\,\psi(\lambda_n,\rho,\beta) \tag{A11}$$

with the functions $\psi(\lambda_n,\rho,\beta)$ defined by the relation

$$-\frac{16\beta}{3\lambda_n^5}\ \psi(\lambda_n,\rho,\beta) = \phi(\lambda_n,\beta)\left[I_0(\lambda_n)\ J_0(\lambda_n\rho) - J_0(\lambda_n)\ I_0(\lambda_n\rho)\right] \tag{A12}$$

where

$$\phi(\lambda_n,\beta) = \frac{N}{I_0(\lambda_n)\, J_0(\lambda_n)\left\{2\lambda_n\left[I_0(\lambda_n)\, J_1(\lambda_n) - I_1(\lambda_n)\, J_0(\lambda_n)\right] - 3I_0(\lambda_n)\, J_0(\lambda_n)\right\}} \tag{A13}$$

and

$$N = \frac{1}{\lambda_n} C_1\, I_0(\lambda_n)\, J_1(\lambda_n) - \frac{1}{\lambda_n} C_1\, J_0(\lambda_n)\, I_1(\lambda_n) + C_2\, I_0(\lambda_n)\left[\frac{1}{\lambda_n} J_1(\lambda_n) - \frac{4}{\lambda_n^3} J_1(\lambda_n) + \frac{2}{\lambda_n^2} J_0(\lambda_n)\right] - C_2\, J_0(\lambda_n)\left[\frac{1}{\lambda_n} I_1(\lambda_n) - \frac{2}{\lambda_n^2} I_0(\lambda_n) + \frac{4}{\lambda_n^3} I_1(\lambda_n)\right]$$

$$+ \frac{1}{2\beta} I_0(\lambda_n) \int_0^1 x e^{-\beta x^2} J_0(\lambda_n x)\, dx - \frac{1}{2\beta} J_0(\lambda_n) \int_0^1 x e^{-\beta x^2} I_0(\lambda_n x)\, dx$$

$$+ I_0(\lambda_n) \int_0^1 x\left(\frac{1}{\beta} + x^2\right) \sum_{m=1}^{\infty} \left[\frac{(-1)^m(\beta x^2)^m}{(2m)m!}\right] J_0(\lambda_n x)\, dx - J_0(\lambda_n) \int_0^1 x\left(\frac{1}{\beta}\right.$$

$$\left. + x^2\right) \sum_{m=1}^{\infty} \left[\frac{(-1)^m(\beta x^2)^m}{(2m)m!}\right] I_0(\lambda_n x)\, dx$$

Phase 1: $0 < t < \tau$

When equations (A4) and (A6) are summed and equation (A11) is used, the velocity during loading, phase 1 ($0 < t < \tau$), becomes

$$v(\rho,t) = -\frac{\sqrt{3}}{4\beta}(F - F')\left[C_1 + C_2\rho^2 + \frac{1}{2\beta} e^{-\beta\rho^2} + \left(\frac{1}{\beta} + \rho^2\right) \sum_{n=1}^{\infty} \frac{(-1)^n(\beta\rho^2)^n}{(2n)n!}\right.$$

$$\left. + \frac{16\beta}{3} \sum_{n=1}^{\infty} \frac{1}{\lambda_n^5} \psi(\lambda_n,\rho,\beta) e^{-(2\lambda_n^4/3\alpha)t}\right] \tag{A14}$$

The displacement of the plate is determined by integrating equation (A14) with respect to time. Taking the initial condition of zero displacement (eqs. (19)) into account, the displacement becomes

APPENDIX

$$\frac{\mu R^2}{\alpha^2 M_o} w(\rho,t) = -\frac{\sqrt{3}}{4\beta\alpha}(F - F')\left\{\left[C_1 + C_2\rho^2 + \frac{1}{2\beta} e^{-\beta\rho^2} + \left(\frac{1}{\beta} + \rho^2\right)\sum_{m=1}^{\infty} \frac{(-1)^m(\beta\rho^2)^m}{(2m)m!}\right]t \right.$$

$$\left. - 8\beta\alpha \sum_{n=1}^{\infty} \frac{1}{\lambda_n^9} \psi(\lambda_n,\rho,\beta)\left(e^{-(2\lambda_n^4/3\alpha)t} - 1\right)\right\} \tag{A15}$$

Phase 2: $\tau < t < t_f$

After the load is removed from the plate at time τ, phase 2 ($\tau < t < t_f$), the governing differential equation becomes

$$\nabla^4 v + \frac{3}{2}\alpha \frac{\partial v}{\partial t} = -2\sqrt{3}F' e^{-\beta\rho^2} \tag{A16}$$

Utilizing the same eigenvalue expansion techniques as before with continuity of velocity from phase 1 to phase 2 produces the plate velocity during phase 2 motion as follows:

$$v(\rho,t) = \frac{\sqrt{3}}{4\beta} F'\left[C_1 + C_2\rho^2 + \frac{1}{2\beta} e^{-\beta\rho^2} + \left(\frac{1}{\beta} + \rho^2\right)\sum_{n=1}^{\infty} \frac{(-1)^n(\beta\rho^2)^n}{(2n)n!}\right]$$

$$-\frac{4}{\sqrt{3}} \sum_{n=1}^{\infty} \frac{1}{\lambda_n^5} \psi(\lambda_n,\rho,\beta)\left[(F - F')e^{-(2\lambda_n^4/3\alpha)\tau} - F\right]e^{-(2\lambda_n^4/3\alpha)(t-\tau)} \tag{A17}$$

Integration of equation (A17) with respect to time with continuity of displacement to determine the arbitrary function of integration produces the displacement of the plate during phase 2 motion as follows:

$$\frac{\mu R^2}{\alpha^2 M_o} w(\rho,t) = \frac{\sqrt{3}}{4\beta\alpha}(F't - F\tau)\left[C_1 + C_2\rho^2 + \frac{1}{2\beta} e^{-\beta\rho^2} + \left(\frac{1}{\beta} + \rho^2\right)\sum_{m=1}^{\infty} \frac{(-1)^m(\beta\rho^2)^m}{(2m)m!}\right]$$

$$+ 2\sqrt{3} \sum_{n=1}^{\infty} \frac{1}{\lambda_n^9} \psi(\lambda_n,\rho,\beta)\left[(F - F')e^{-(2\lambda_n^4/3\alpha)t} - Fe^{-(2\lambda_n^4/3\alpha)(t-\tau)} + F'\right] \tag{A18}$$

Equations (A14), (A15), (A17), and (A18) represent the complete solution for the velocity and displacement of the plate. In the limit as β approaches 0, the Gaussian distribution becomes the uniform distribution of load and this solution reduces to the solution presented by Wierzbicki (ref. 15).

REFERENCES

1. Perzyna, Piotr: Dynamic Load Carrying Capacity of a Circular Plate. Arch. Mech. Stosow., vol. 10, no. 5, 1958, pp. 635-647.

2. Weidman, Deene J.: Response of a Plastic Circular Plate to a Distributed Time-Varying Loading. Ph.D. Thesis, Virginia Polytech. Inst. & State Univ., 1968.

3. Youngdahl, Carl K.: Influence of Pulse Shape on the Final Plastic Deformation of a Circular Plate. Int. J. Solids & Struct., vol. 7, no. 9, Sept. 1971, pp. 1127-1142.

4. Florence, Alexander L.: Annular Plate Under a Transverse Line Impulse. AIAA J., vol. 3, no. 9, Sept. 1965, pp. 1726-1732.

5. Florence, A. L.: Clamped Circular Rigid-Plastic Plates Under Central Blast Loading. Int. J. Solids & Struct., vol. 2, no. 2, Apr. 1966, pp. 319-335.

6. Sneddon, Ian N.: Fourier Transforms. First ed., McGraw-Hill Book Co., Inc., 1951.

7. Madden, Richard: Ballistic Limit of Double-Walled Meteoroid Bumper Systems. NASA TN D-3916, 1967.

8. Thomson, Robert G.: Plastic Behavior of Circular Plates Under Transverse Impulse Loadings of Gaussian Distribution. NASA TR R-279, 1968.

9. Hayduk, Robert J.: Gaussian Ideal Impulsive Loading of Rigid Viscoplastic Plates. Advances in Engineering Science - Volume 2, NASA CP-2001, [1976], pp. 595-616.

10. Lepik, Yu R.: On the Dynamical Flexure of Infinite Plastic-Rigid Plates. Sov. Appl. Mech., vol. 10, no. 6, June 1974, pp. 615-619.

11. Perzyna, Piotr: The Constitutive Equations for Work-Hardening and Rate Sensitive Plastic Materials. Proc. Vib. Probl., Inst. Basic Tech. Probl., Polish Acad. Sci., vol. 4, no. 3, 1963, pp. 281-290.

12. Hohenemser, K.; and Prager, W.: Mechanics of Isotropic Media. Z. Angew. Math. & Mech., Bd. 12, Aug. 1932, pp. 216-226.

13. Prager, W.: Mécanique des Solides Isotropes au delà du Domaine Élastique. Mem. Sci. Math., fasc. LXXXVII, 1937.

14. Perzyna, P.: Fundamental Problems in Viscoplasticity. Adv. Appl. Mech., vol. 9, 1966, pp. 202-243.

15. Wierzbicki, T.: Impulsive Loading of Rigid Viscoplastic Plates. Int. J. Solids & Struct., vol. 3, no. 4, July 1967, pp. 635-647.

16. Wierzbicki, T.: A Method of Approximate Solution of Boundary Value Problems for Rigid, Viscoplastic Structures. Acta Mech., vol. III, no. 1, 1967, pp. 56-66.

17. Florence, A. L.: Circular Plate Under a Uniformly Distributed Impulse. Int. J. Solids & Struct., vol. 2, no. 1, Jan. 1966, pp. 37-46.

18. Hayduk, Robert J.; and Thomson, Robert G.: Static Load-Carrying Capacity of Circular Rigid-Plastic Plates Under Gaussian Distribution of Pressure. Int. J. Solids & Struct., vol. 12, no. 8, 1976, pp. 555-558.

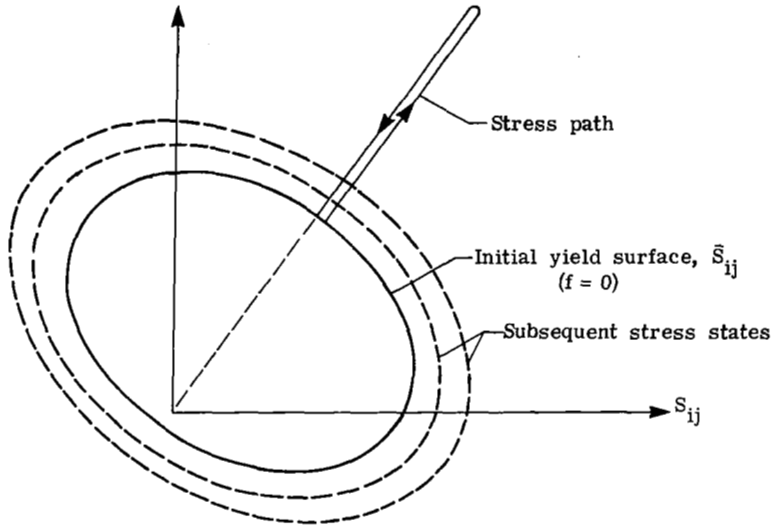

Figure 1.- Representation of proportional loading in deviatoric stress space.

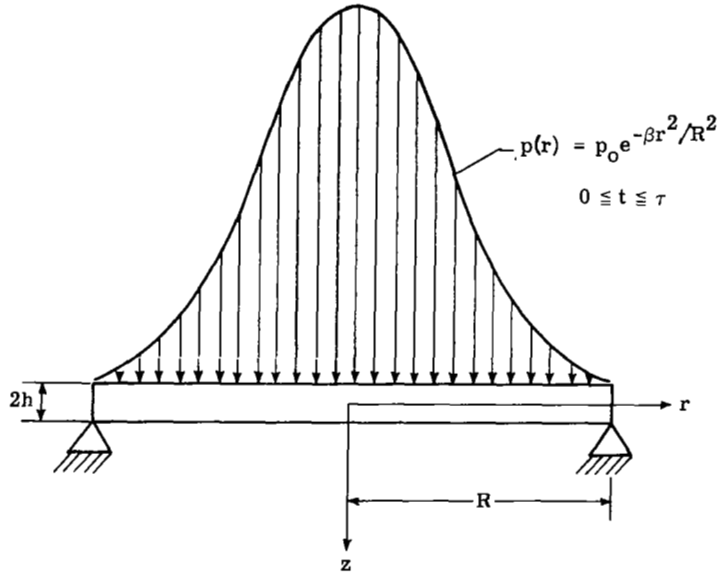

Figure 2.- Simply supported circular plate with Gaussian distribution of pressure applied during time interval τ.

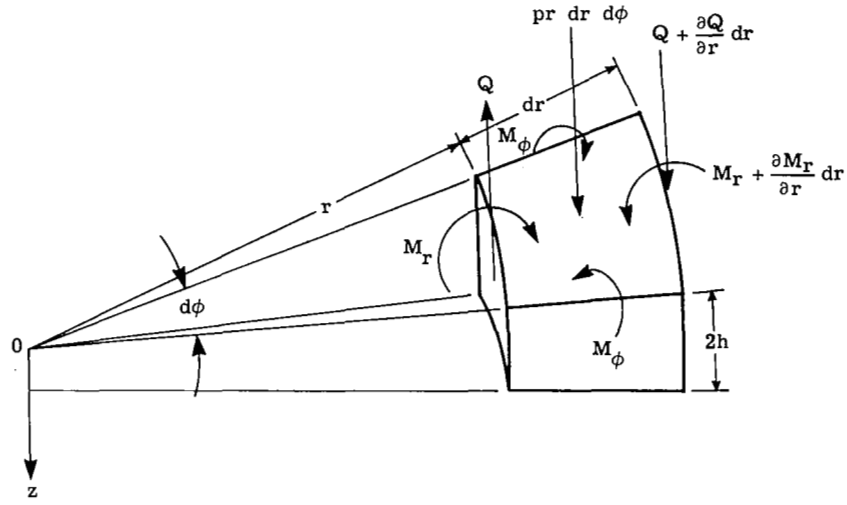

Figure 3.- Element of circular plate with applied forces and moments.

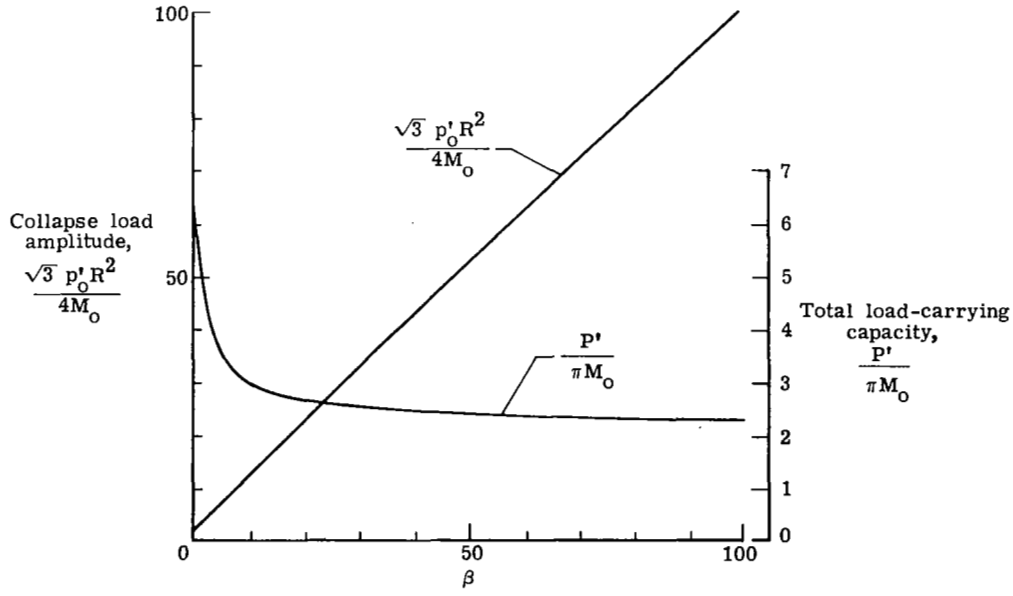

Figure 4.- Nondimensional collapse load amplitude and total load-carrying capacity as functions of load distribution parameter β.

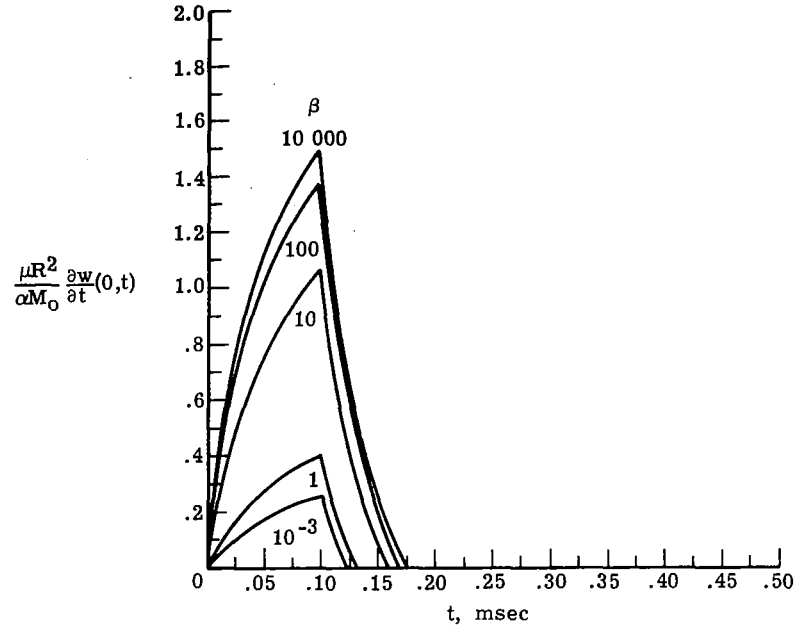

(a) $\alpha = 1 \times 10^{-3}$ sec.

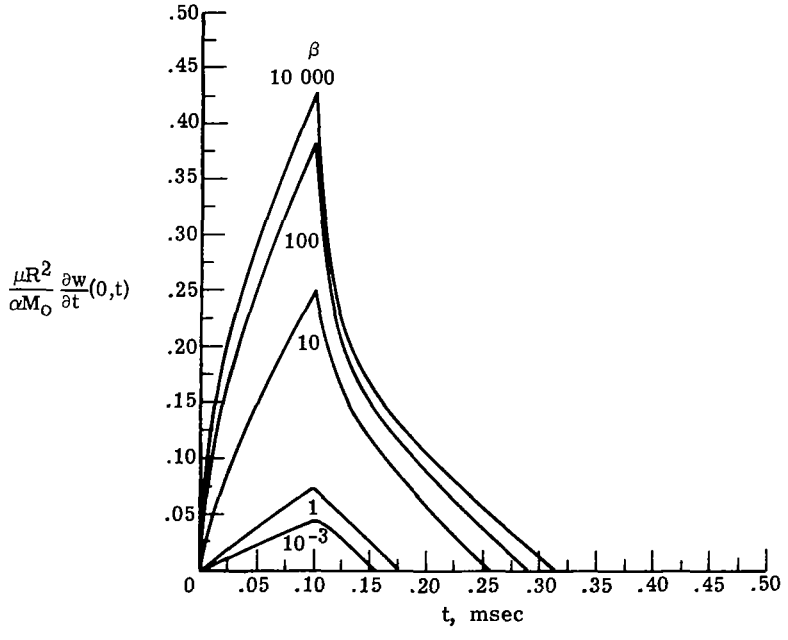

(b) $\alpha = 1 \times 10^{-2}$ sec.

Figure 5.- Time history of plate central velocity for various values of shape parameter β.

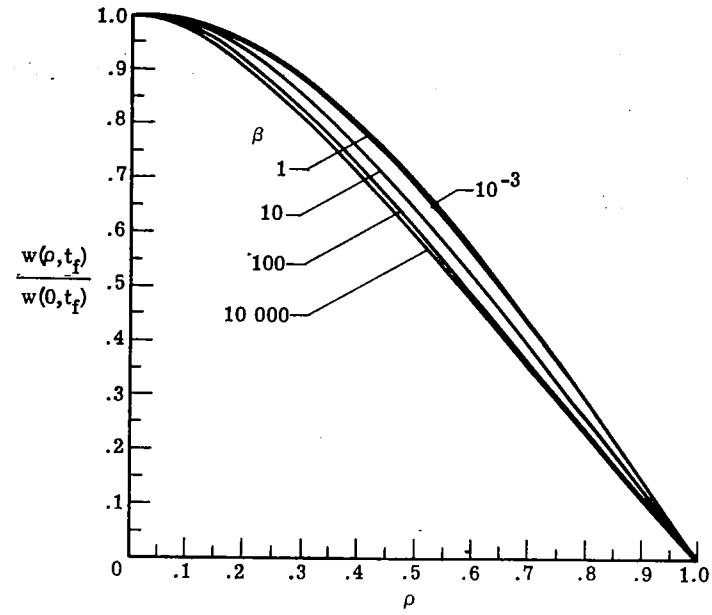

(a) $\alpha = 1 \times 10^{-3}$ sec.

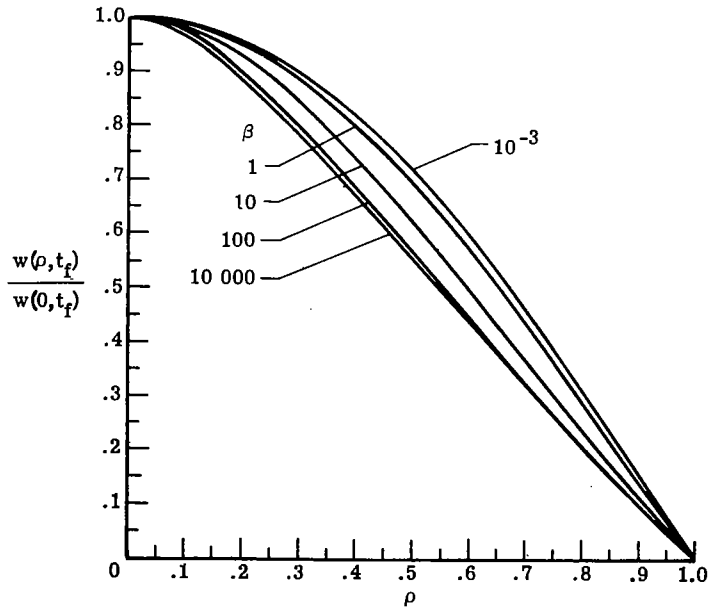

(b) $\alpha = 1 \times 10^{-2}$ sec.

Figure 6.- Final plate profiles for various values of shape parameter β.

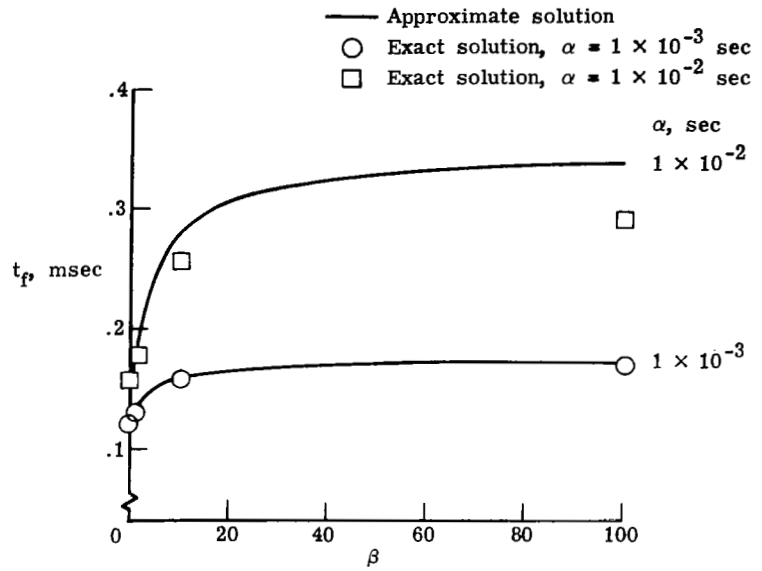

Figure 7.- Comparison of approximate expression (eq. (22)) for time for motion to cease t_f and points determined from complete equations for step-pressure loading.

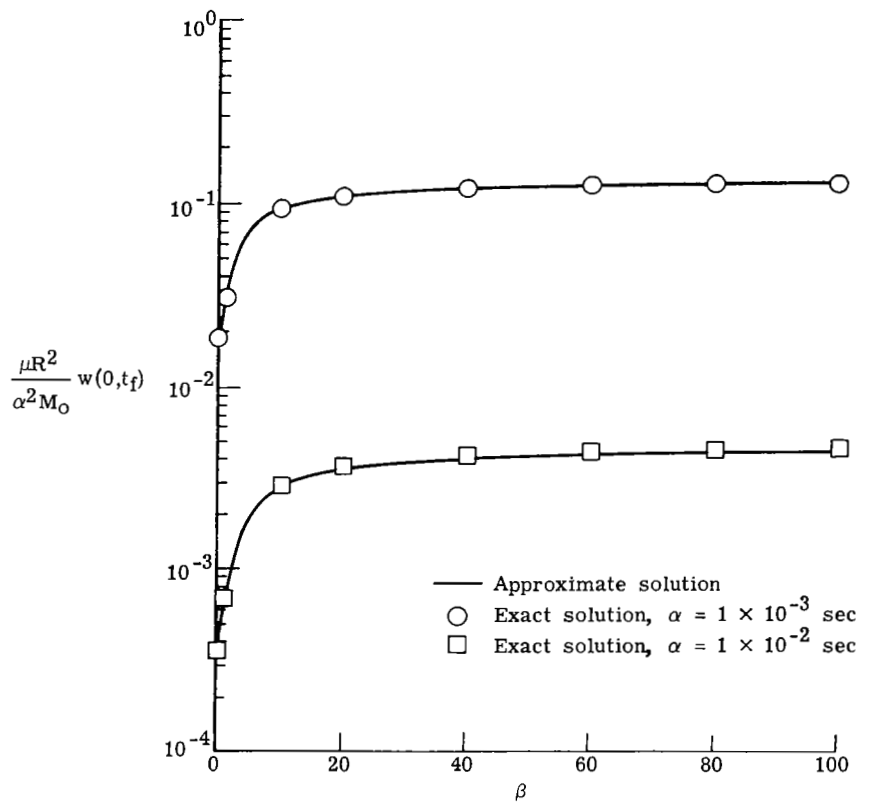

Figure 8.- Comparison of approximate expression (eq. (24)) for final central deflection and points determined from complete equations for step-pressure loading.

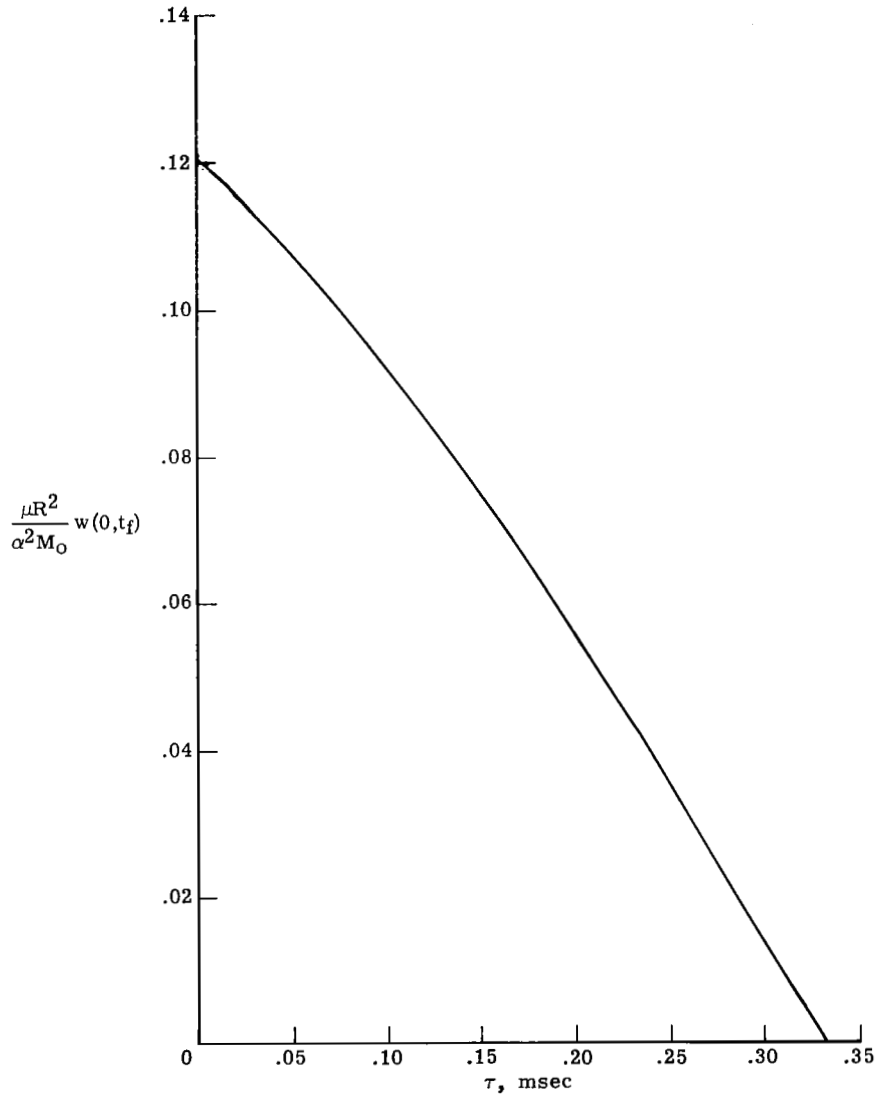

Figure 9.- Variation of final center displacement with load duration. Total impulse held constant; $\alpha = 1 \times 10^{-3}$ sec; $\beta = 10$.

1. Report No. NASA TP-1123	2. Government Accession No.	3. Recipient's Catalog No.
4. Title and Subtitle GAUSSIAN STEP-PRESSURE LOADING OF RIGID VISCOPLASTIC PLATES		5. Report Date March 1978
		6. Performing Organization Code
7. Author(s) Robert J. Hayduk and Barbara J. Durling		8. Performing Organization Report No. L-11885
		10. Work Unit No. 505-02-13-01
9. Performing Organization Name and Address NASA Langley Research Center Hampton, VA 23665		11. Contract or Grant No.
		13. Type of Report and Period Covered Technical Paper
12. Sponsoring Agency Name and Address National Aeronautics and Space Administration Washington, DC 20546		14. Sponsoring Agency Code

15. Supplementary Notes

Part of the information presented in this report was included in a thesis submitted by Robert J. Hayduk in partial fulfillment of the requirements for the Degree of Doctor of Philosophy in Engineering Mechanics, Virginia Polytechnic Institute and State University, Blacksburg, Va., Aug. 1972.

16. Abstract

The response of a thin, rigid viscoplastic plate subjected to a spatially axisymmetric Gaussian step-pressure impulse loading was studied analytically. A Gaussian pressure distribution in excess of the collapse load is applied to the plate, is held constant for a length of time, and then is suddenly removed. The plate deforms with monotonically increasing deflections until the dynamic energy is completely dissipated in plastic work. The simply supported plate of uniform thickness obeys the von Mises yield criterion and a generalized constitutive equation for rigid viscoplastic materials. For the small deflection bending response of the plate, the governing system of equations is essentially nonlinear. Transverse shear stress is neglected in the yield condition and rotary inertia in the equations of dynamic equilibrium. A proportional loading technique, known to give excellent approximations of the exact solution for the uniform load case, was used to linearize the problem and to obtain the analytical solutions in the form of eigenvalue expansions. The effects of load concentration, of an order of magnitude change in the viscosity of the plate material, and of load duration were examined while holding the total impulse constant.

17. Key Words (Suggested by Author(s))	18. Distribution Statement
Viscoplasticity Plates Impulse loading Gaussian loading Bending response	Unclassified - Unlimited Subject Category 39

19. Security Classif. (of this report)	20. Security Classif. (of this page)	21. No. of Pages	22. Price*
Unclassified	Unclassified	25	$4.00

* For sale by the National Technical Information Service, Springfield, Virginia 22161

NASA-Langley, 1978